Harmonic Lattice Behavior of Two-Dimensional Colloidal Crystals

P. Keim, G. Maret, U. Herz, and H. H. von Grünberg

Fachbereich Physik, Universität Konstanz, P.O.B. 5560, 78457 Konstanz, Germany

(Received 13 February 2004; published 27 May 2004)

Using positional data from videomicroscopy and applying the equipartition theorem for harmonic Hamiltonians, we determine the wave-vector-dependent normal mode spring constants of a two-dimensional colloidal model crystal and compare the measured band structure to predictions of the harmonic lattice theory. We find good agreement for both the transversal and the longitudinal modes. For $q \to 0$, the measured spring constants are consistent with the elastic moduli of the crystal.

DOI: 10.1103/PhysRevLett.92.215504 PACS numbers: 61.66.–f, 63.20.Dj, 82.70.Dd

Colloidal crystals have a long tradition as condensed matter analogs of ordinary solids. They are studied, for example, to understand phenomena such as freezing and melting [1]. Unlike in ordinary solids having properties that are often difficult to connect to the underlying atomic interactions, the interparticle potentials in such colloidal crystals are in most cases precisely known and, more importantly, externally controllable. Moreover, the relevant time and length scales in colloidal systems are comparatively easy to access experimentally. Both aspects suggest studies directly probing the connection between microscopic interaction potentials and macroscopic crystal properties.

The property we here consider is the crystal's elastic response to thermal excitations, specifically the phonon elastic dispersion relations. In this regard, colloidal crystals are rather special in that their phonons are almost always overdamped: The ratio between the wave-vector dependent frequency $\omega(\vec{q}) = \sqrt{\lambda(\vec{q})/m}$, characteristic of the harmonic forces with spring constants $\lambda(\vec{q})$, and the friction factors $\Lambda(\vec{q})$ (also q dependent [2]) for the modes of lattice motion through the host liquid is typically of the order of 10^{-3} to 10^{-4} in colloidal systems. Therefore, the time autocorrelation function of a phonon normal mode coordinate decays exponentially with a rate given by $\lambda(\vec{q})/\Lambda(\vec{q})$ [2,3]. This decay rate can be, and has repeatedly been, measured by means of dynamical light scattering [2,4–7] or inelastic light scattering [8]. Phonon-dispersion relations have been determined in charge stabilized [2,5,6] and purely hard sphere colloidal crystals [7,8], in the context of dusty plasma physics [9], but also in more exotic systems such as crystals made of mm steel spheres [10] or optically anisotropic spheres [4]. Microscopic information about the spring constants and thus the particle interaction potentials can be derived only from these decay rates, i.e., from $\lambda(\vec{q})/\Lambda(\vec{q})$, if one resorts to a model describing the complicated frictional and hydrodynamical forces. A direct access to $\lambda(\vec{q})$, i.e., one free from any assumptions of a model, is not possible in this approach.

In this Letter, we report on a videomicroscopy study of two-dimensional (2D) colloidal crystals and show how to obtain direct access to the normal mode band structure $\lambda(\vec{q})$ of the crystal, circumventing, in particular, the difficulties arising from the hydrodynamic interactions. The central idea is to avoid a dynamical measurement and to analyze instead spatial correlations between the particles which are then related to the $\lambda(\vec{q})$, the eigenvalues of the dynamical matrix characterizing the elastic properties of the harmonic crystal. This becomes possible through the use of digital videomicroscopy [11] providing us with the trajectories of all particles. The colloidal system we examine is well studied and the interparticle potential precisely known [12–14]. This will be of advantage when establishing a quantitative link between the measured $\lambda(\vec{q})$ and the theoretical band structure based on the pair potential.

The experimental setup is an improved version of the one described in [12]: Spherical colloids (diameter $d = 4.5\ \mu$m) are confined by gravity to a water/air interface formed by a water drop suspended by surface tension in a top sealed cylindrical hole of a glass plate. The flatness of the interface can be controlled within $\pm\frac{1}{2}\ \mu$m. The field of view has a size of $835\ \mu\text{m} \times 620\ \mu$m containing typically up to 3×10^3 particles, whereas the whole sample contains about 10^5 particles. The number of particles in the field of view is controlled by the curvature of the droplet via an active regulation with an accuracy of 1% and the biggest observed particle-density gradient is 0.7%. The variation of the inclination of the sample is in the range of $\alpha \approx 1\ \mu$rad so that the collective motion of the particles relative to the field of view is below $2\ \mu$m/h providing best equilibrium conditions for long time stability. The particles are superparamagnetic due to Fe_2O_3 doping. A magnetic field $\vec{B}$ applied perpendicular to the air/water interface induces in each particle a magnetic moment $\vec{M} = \chi\vec{B}$ which leads to a repulsive dipole-dipole pair-interaction energy of $\beta v(r) = \Gamma/(\sqrt{\pi\rho}r)^3$ with the dimensionless interaction strength given by $\Gamma = \beta(\mu_0/4\pi)(\chi B)^2(\pi\rho)^{3/2}$ ($\beta = 1/kT$ inverse temperature, χ susceptibility, $\rho = 2/\sqrt{3}a^2$ 2D density, a lattice constant of a hexagonal lattice). The interaction can be externally controlled by means of the magnetic field B. Γ was determined as in Ref. [12] and is the only parameter

controlling the phase behavior of the system. For $\Gamma > 60$, the sample is a hexagonal crystal [13] (see Fig. 1). The sample was tempered at high interaction strength up to $\Gamma = 250$ deep in the crystalline phase until a 2D monocrystal was observed. We here analyze three different crystals, from hard to soft ($\Gamma = 250$, 175, 75), and use for each system about 2000 statistically independent configurations with approximately 1300 particles, recorded at equal time intervals ($\Delta t = 2$ s) in a 440 μm $\times$ 440 μm frame using digital videomicroscopy with subsequent image processing on the computer. For each of all N particles in a given configuration, we determine the displacement $\vec{u}(\vec{R})$ of the particle from its equilibrium position $\vec{R}$.

Using the theory of harmonic crystals [15], we now derive an equation guiding us from the measured displacement vectors $\vec{u}(\vec{R})$ to the eigenvalues of the dynamical matrix. Let $D_{\mu,\nu}(\vec{q})$ ($\mu, \nu \in \{x, y\}$) be the dynamical matrix [15], connected through a Fourier transformation to the matrix $D_{\mu,\nu}(\vec{R}, \vec{R}')$ which is essentially the matrix of the second derivatives of the pair potential $v(r) \sim \Gamma/r^3$. It is obvious that $D_{\mu,\nu}(\vec{q})$ depends linearly on the interaction strength parameter Γ; therefore we write $D_{\mu,\nu}(\vec{q}) = (kT\Gamma/a^2)\tilde{D}_{\mu,\nu}(\vec{q})$ and obtain the dimensionless dynamical matrix $\tilde{D}_{\mu,\nu}(\vec{q})$ which is independent of Γ. Its eigenvalues are denoted by $\lambda_s(\vec{q})a^2/(kT\Gamma)$. Here the polarization subscript s stands for the longitudinal ($s = l$) and transversal ($s = t$) mode. The harmonic potential energy of the crystal can be written in the following form [15]:

$$U = \frac{1}{2}\sum_{\vec{q},\mu,\nu} u^*_\mu(\vec{q}) D_{\mu,\nu}(\vec{q}) u_\nu(\vec{q}), \tag{1}$$

with $u_\nu(\vec{q})$ being the νth component of the Fourier transform of the displacement vectors $\vec{u}(\vec{R})$. The equipartition theorem for a classical harmonic Hamiltonian states that,

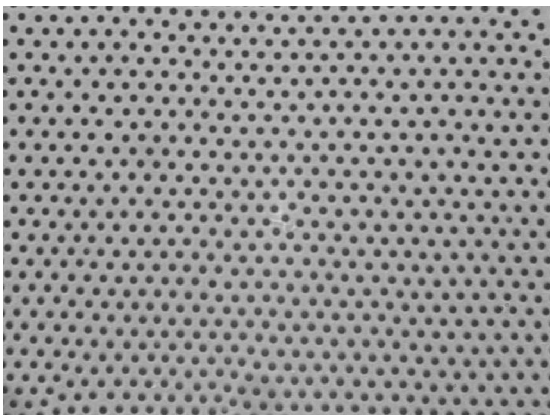

FIG. 1. Micrograph (420 μm $\times$ 310 μm) of a typical colloidal crystal investigated in the present work; the two-dimensional system consists of paramagnetic colloids confined at the air-water interface of a hanging water drop.

on average, every mode has an energy of $kT/2$. Thus, $\langle u^*_\mu(\vec{q}) D_{\mu,\nu}(\vec{q}) u_\nu(\vec{q})\rangle/2 = kT/2$ and this leads us to [16]

$$\langle u^*_\mu(\vec{q}) u_\nu(\vec{q})\rangle = kT D^{-1}_{\mu,\nu}(\vec{q}), \tag{2}$$

where in our case the average has to be taken over all measured configurations. Introducing with $p_s(\vec{q})$ an abbreviation for the eigenvalues of the matrix $\Gamma\langle u^*_\mu(\vec{q}) u_\nu(\vec{q})\rangle/a^2$, one arrives at

$$\frac{1}{p_s(\vec{q})} = \frac{\lambda_s(\vec{q})a^2}{kT\Gamma}, \qquad (s = t, l). \tag{3}$$

Static and slowly moving distortions of the lattice are the main source of error in our experiment. We sometimes observe long-range bending of lattice lines, a finite-size problem which in soft crystals can be partly overcome in giving the crystal enough time to equilibrate. This takes more time, the harder the crystal. For our hardest crystal, we have not managed to avoid a small but clearly visible bending of lines. A second problem is related to the determination of each particle's equilibrium position $\vec{R}$, without which the displacement vectors $\vec{u}(\vec{R})$ cannot be determined. A cooperative drift of all particles can be observed: Particles can depart significantly from their lattice sites, but keep a nearly constant distance from each other so that nearby trajectories are similar (illustrative example pictures of these trajectories can be found in [13,17]). This is a behavior typical of a 2D crystal. It is long known [18] that no true long-range order exists in 2D crystals. In contrast to a 3D crystal, the density-density correlation function decays algebraically with distance and the root mean square displacement diverges logarithmically with system size. The answer to this problem is the introduction of a "local" coordinate system; that is, one in which the particles' displacement is calculated with respect to the positions of nearest neighbors [17,19]. Then, the root mean square displacement stays indeed finite, and the 2D crystal melts as predicted by Lindemann's rule [17]. This has been confirmed also experimentally [13]. To correct our data for this long-range distortion, we first calculated coarse-grained trajectories by averaging over a sliding time window ΔT having a width of 25, 40, and 60Δt for $\Gamma = 250$, 175, and 75, respectively. We then analyzed the short-time displacement of the particles with respect to these coarse-grained trajectories to obtain the true fluctuations of the underlying crystal. Our whole data evaluation procedure has been successfully tested by processing data obtained from Monte Carlo simulations, using the pair potential and parameters of our experiment.

Figure 2 shows $1/p_s(\vec{q})$ from Eq. (3) as obtained from the measured set of displacement vectors for $\Gamma = 250$, 175, and 75, and compares it to the theoretical band structure (solid lines) of a harmonic crystal having a two-dimensional hexagonal lattice ($a = 12.98$ μm). The latter is based on the second derivatives of the known pair

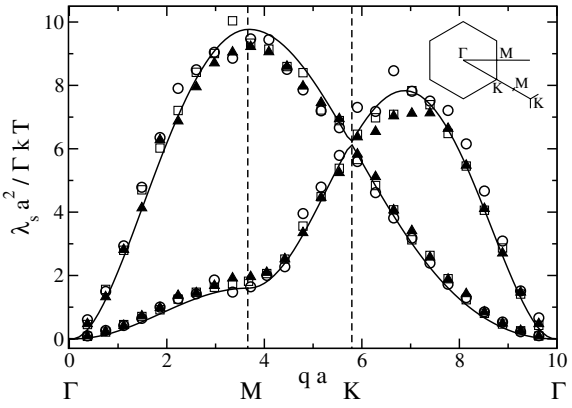

FIG. 2. Band structure of harmonic lattice spring constants of a 2D colloidal crystal. Symbols for constants experimentally determined with Eqs. (2) and (3) from the relative displacement of the particles from their equilibrium position for a soft ($\Gamma = 75$, empty circles), a hard ($\Gamma = 175$, empty squares), and a very hard ($\Gamma = 250$, filled triangles) crystal; solid lines for the theoretical band structure calculated from standard harmonic crystal theory using the pair potential $\beta v(r) = \Gamma/(\sqrt{\pi\rho}r)^3$. The inset shows the first Brillouin zone of the hexagonal lattice and labels for high-symmetry points, defining the lines in the interior and on the surface of the first Brillouin zone along which the band structure is plotted. The upper curve corresponds to the longitudinal, and the lower one to the transversal mode.

potential and results from diagonalizing $\tilde{D}_{\mu,\nu}(\vec{q})$ [15]. 17 neighbor shells have been taken into account in $D_{\mu,\nu}(\vec{R}, \vec{R}')$; the difference to the results for only three shells is already tiny. We find good agreement for both the transversal and longitudinal mode. No fit parameter has been used. Preaveraging with a finite time window improves the agreement. Without it (i.e., taking the average over the whole trajectory to define $\vec{R}$), the peak at the M point in the band structure is about 10% smaller for each Γ than it is in Fig. 2. The data are particularly sensitive to the quality of the crystal near the edges of the first Brillouin zone, especially near the M point. The uncertainty in determining the direction of the lattice lines plus the bending of these lines explain the remaining differences between the theoretical and the experimental band structure, but also the differences between the three different crystals. We also checked for the occurrence of dislocations in all our samples. Only thermally activated dislocation pairs have been observed, but no static, isolated dislocation destroying the crystal symmetry.

At $q \to 0$, the elastic moduli of the crystal can be read off from the elastic dispersion curves: $\lim_{q\to 0}\lambda_t(\vec{q}) = \mu v_0 q^2$ and $\lim_{q\to 0}\lambda_l(\vec{q}) = (K + \mu)v_0 q^2$, where K and μ are the bulk and shear elastic moduli of continuum theory (with the cell volume $v_0 = 1/\rho$). Moreover, in the elastic limit $\lambda_l(\vec{q})$ and $\lambda_t(\vec{q})$ are particularly simple to obtain from the measured displacement vectors: We multiply on either side of Eq. (2) $\vec{q}_\parallel = (q_x, q_y)$ and $\vec{q}_\perp = (-q_y, q_x)$ from the left and the right, to find

$$d_i(\vec{q}) \equiv \frac{v_0}{a^2}\langle|\vec{q}_i\vec{u}(\vec{q})|^2\rangle = \frac{kTv_0}{a^2}\sum_{\mu,\nu} q_{i,\mu}D^{-1}_{\mu,\nu}(\vec{q})q_{i,\nu}, \quad i = \parallel, \perp . \tag{4}$$

which are the radial and azimuthal projection of the Fourier transform of the displacement vectors onto $\vec{q}$. These projections are now directly related to the inverse of the elastic moduli: $\lim_{q\to 0} d_\parallel(\vec{q}) = kT/((K + \mu)a^2)$ and $\lim_{q\to 0} d_\perp(\vec{q}) = kT/(\mu a^2)$. Since $D_{\mu,\nu}(\vec{q})$ depends linearly on Γ, the quantity $\Gamma d_i(\vec{q})$ ($i = \parallel, \perp$) is independent of Γ. Figure 3 shows $d_\parallel(\vec{q})\Gamma$ and $d_\perp(\vec{q})\Gamma$, evaluated with the experimental data for all three crystals ($\Gamma = 75$, 175, 250 symbols) and theoretically using the dynamical matrix $D_{\mu,\nu}(\vec{q})$ and the pair potential (solid lines). For the pair potential $\sim\Gamma/r^3$, the elastic constants can be calculated to be $Ka^2/kT = 3.461\Gamma$ and $\mu = K/10$ in the limit $\Gamma \to \infty$ ($T = 0$) [14,20]. Arrows in Fig. 3 indicate the prediction of the $T = 0$ calculation. While the data on the longitudinal branch [curves (3) and (4)] show excellent agreement and correctly approach the $T = 0$ inverse bulk modulus, theoretical and experimental data on the transversal branch disagree at low q. This is due to the time windowing of our data and the finite size of our sample. Taking data from this very experiment, it has already been shown [14] that appropriate finite-size scaling leads to an almost perfect agreement with the $T = 0$ prediction of the elastic moduli. We should also remark that the location of the branching points of the $\Gamma \to K$ and $\Gamma \to M$ curves in Fig. 3 reveal that the assumption of isotropy is justified only if $qa < 1$ for the transversal and

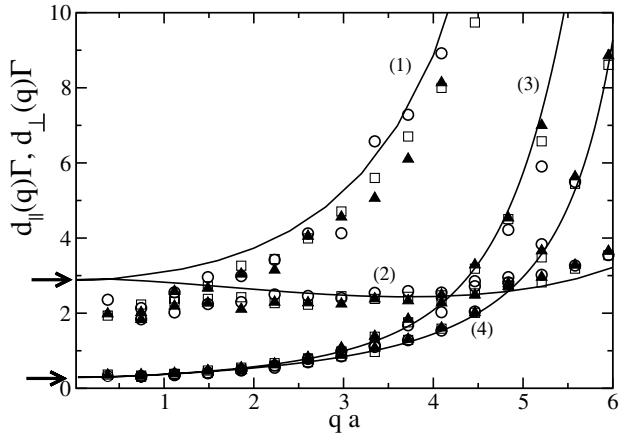

FIG. 3. $d_\parallel(\vec{q})\Gamma$ and $d_\perp(\vec{q})\Gamma$ from Eq. (4), evaluated with the same data as in Fig. 2. For $q \to 0$, $d_\parallel(\vec{q}) \to kT/((K + \mu)a^2)$ and $d_\perp(\vec{q}) \to kT/(\mu a^2)$, where K is the bulk modulus and μ the shear modulus. Curves (1) and (2) are $d_\perp(\vec{q})\Gamma$ in the $\Gamma \to M$ [curve (1)] and the $\Gamma \to K$ [curve (2)] directions, (3) and (4) are $d_\parallel(\vec{q})\Gamma$ in the $\Gamma \to K$ [curve (3)] and the $\Gamma \to M$ [curve (4)] directions. Symbols, lines, and the labels Γ, K, M for symmetry points are all defined in Fig. 2. Arrows indicate the $T = 0$ prediction of the elastic moduli (see text).

$qa < 3$ for the longitudinal modes. This defines the limits for the continuum approach often chosen to describe this system.

In summary, we used videomicroscopy data to determine $\vec{q}$-dependent normal mode spring constants of a 2D colloidal crystal. We checked the continuum limit and compared the experimental data to the predictions of the classical theory of a harmonic crystal. Our data evaluation procedure can be seen as an illustration of the validity of the equipartition theorem. The success of our undertaking was not clear from the beginning; if a crystal in 2D is not stable, how can one measure the normal mode spring constants? Here the ideas put forward in [13,17] proved helpful, specifically the introduction of a local coordinate system. Analyzing particle distributions at equilibrium, we were allowed to completely ignore the lattice dynamics. In this context, it is worth remembering that Fig. 2 is not a phonon-dispersion relation in the classical sense as there are no phonons propagating with $\omega_s(\vec{q}) = \sqrt{\lambda_s(\vec{q})/m}$. Our results demonstrate that a colloidal crystal can be seen as a bead-spring lattice immersed in a viscous fluid [21]. A normal vibration mode then transforms into a "normal relaxation mode" [2,21], and the motion of a particle is to be understood as superposition of these "normal relaxation modes." A time-dependent analysis of our data will allow one to study the relaxation process of these normal modes. These avenues await further investigations. We finally remark that the statics and dynamics of overdamped phonons in two-dimensional colloidal crystals may also be seen as a contribution to our understanding of surface phonons [22].

Stimulating discussions with R. Klein and E. Trizac are gratefully acknowledged. We also acknowledge financial support from the Deutsche Forschungsgemeinschaft (European Graduate College "Soft Condensed Matter" and Schwerpunktprogramm Ferrofluide, SPP 1104).

[1] A. K. Sood, Solid State Phys. Adv. Res. Appl. **45**, 1 (1991); A. K. Arora and B. V. R. Tata, *Ordering and Phase Transitions in Charged Colloids* (VCH, New York, 1995); H. Löwen, Phys. Rep. **237**, 76 (1994).

[2] A. J. Hurd, N. A. Clark, R. C. Mockler, and W. J. O'Sullivan, Phys. Rev. A **26**, 2869 (1982); A. J. Hurd, N. A. Clark, R. C. Mockler, and W. J. O'Sullivan, J. Fluid Mech. **153**, 401 (1985).

[3] J. M. A. Hofman, H. J. H. Clercx, and P. P. J. M. Schram, Physica (Amsterdam) **268A**, 353 (1999).

[4] R. Piazza and V. Degiorgio, Phys. Rev. Lett. **67**, 3868 (1991).

[5] J. Derksen and W. van de Water, Phys. Rev. A **45**, 5660 (1992).

[6] M. Hoppenbrouwers and W. van de Water, Phys. Rev. Lett. **80**, 3871 (1998).

[7] Z. D. Cheng, J. X. Zhu, W. B. Russel, and P. M. Chaikin, Phys. Rev. Lett. **85**, 1460 (2000).

[8] R. S. Penciu, M. Kafesaki, G. Fytas, E. N. Economou, W. Steffen, A. Hollingsworth, and W. B. Russel, Europhys. Lett. **58**, 699 (2002); R. S. Penciu, H. Kriegs, G. Petekidis, G. Fytas, and E. N. Economou, J. Chem. Phys. **118**, 5224 (2003).

[9] P. P. J. M. Schram and S. A. Trigger, Contrib. Plasma Phys. **41**, 219 (2001); S. Nunomura, S. Zhdanov, G. E. Morfill, and J. Goree, Phys. Rev. E **68**, 026407 (2003); S. Zhdanov, S. Nunomura, D. Samsonov, and G. Morfill, Phys. Rev. E **68**, 035401(R) (2003).

[10] M. B. Hay, R. K. Workman, and S. Manne, Phys. Rev. E **67**, 012401 (2003).

[11] C. A. Murray and D. G. Grier, Annu. Rev. Phys. Chem. **47**, 421 (1996)

[12] K. Zahn, J. M. Mendez-Alcaraz, and G. Maret, Phys. Rev. Lett. **79**, 175 (1997); K. Zahn, R. Lenke, and G. Maret, Phys. Rev. Lett. **82**, 2721 (1999); K. Zahn, G. Maret, C. Ruß, and H. H. von Grünberg, Phys. Rev. Lett. **91**, 115502 (2003).

[13] K. Zahn and G. Maret, Phys. Rev. Lett. **85**, 3656 (2000).

[14] K. Zahn, A. Wille, G. Maret, S. Sengupta, and P. Nielaba, Phys. Rev. Lett. **90**, 155506 (2003).

[15] N. W. Ashcroft and N. D. Mermin, *Solid State Physics* (Saunders College, Philadelphia, 1976), Chap. 22.

[16] P. M. Chaikin and T. C. Lubensky, *Principles of Condensed Matter Physics* (Cambridge University Press, Cambridge, England, 1995), p. 223.

[17] X. H. Zheng and J. C. Earnshaw, Europhys. Lett. **41**, 635 (1998).

[18] N. D. Mermin, Phys. Rev. **176**, 250 (1968).

[19] V. M. Bedanov and G. V. Gadiyak, Phys. Lett. A **109**, 289 (1985).

[20] A. Wille, Ph.D. thesis, University of Konstanz, Konstanz, Germany, 2001.

[21] Y. N. Ohshima and I. Nishio, J. Chem. Phys. **114**, 8649 (2001).

[22] W. Kress and F. W. de Wette, *Surface Phonons* (Springer-Verlag, Berlin, Heidelberg, 1991).